OPEN

Value of the Cinematic Rendering From Volumetric Computed Tomography Data in Evaluating the Relationship Between Deep Soft Tissue Sarcomas of the Extremities and Adjacent Major Vessels: A Preliminary Study

Kun Li, MD, Ruiying Yan, MD, Huan Ma, MD, Da-fu Zhang, MD, Yingying Ding, MD, and Zhen-hui Li, MD, PhD

Objective: The aim of the study was to assess the value of cinematic rendering (CR) from volumetric computed tomography data in evaluating the relationship between deep soft tissue sarcomas (STSs) of the extremities and the adjacent major vessels.

Methods: Preoperative contrast-enhanced axial imaging (CEAI) in the arterial phase with three-dimensional volume rendering (VR) and CR of contrast-enhanced computed tomography were used to assess adjacent vascular invasion in 43 cases of deep STSs of the extremities. The imaging assessments were compared with surgical findings and interpreted as negative (no vascular invasion) or positive (vascular invasion was present). Intrareader and interreader agreement were assessed using Cohen κ statistics. The diagnostic performance of CEAI, VR, and CR was evaluated by receiver operating curve analysis and compared using the DeLong test.

Results: Thirty-four and nine cases were classified as negative and positive, respectively, in surgery. Intrareader agreement values for the CEAI, VR, and CR assessments were all excellent (0.984, 0.934, and 0.914, respectively), whereas the interreader agreement for CEAI assessments was greater than that for VR and CR (0.969 vs 0.804 and 0.761). Cinematic rendering showed lower accuracy (0.698), sensitivity (0.778), specificity (0.676), positive predictive values (0.389), and negative predictive values (0.920) for vascular invasion diagnosis than CEAI or VR; the accuracy, sensitivity, specificity, positive predictive values, and negative predictive values increased to 0.767, 0.889, 0.735, 0.471, and 0.962 for both CEAI and VR. The results were not statistically significant (all $P > 0.05$).

Conclusions: Cinematic rendering has the potential to be used to evaluate vascular invasion in cases of deep STSs of the extremities, but it should be used alongside the traditional methods such as CEAI.

Key Words: contrast enhanced CT, volume rendering, cinematic rendering, soft tissue sarcoma

Soft tissue sarcomas are a group of rare malignant tumors originating from connective tissues. They can occur at any age and in any anatomic site.[1] These tumors are challenging to diagnose and treat because of the high degree of malignancy, multiple pathological subtypes, and heterogeneity in biological properties; the disease may also relapse easily or show distant metastasis.[1] Regardless of the pathological type and grade, surgery is still the most effective method for the treatment of soft tissue sarcomas (STSs) except gastrointestinal stromal tumors and desmoid.[2] The presence of osseous, joint, nerve, and vascular invasion are largely determinant of the feasibility of limb sparing surgery. When STSs, especially deep tumors, involve the major vessels, limb salvage may not be possible for main surgical solutions.[3] The choice of the treatment strategy for STSs is often difficult, but standardized surgical resection can increase the local control rate of the STS and improve the limb salvage rate. Therefore, accurate delineation of the local extent of the neoplasm in bones, muscles, and joints is essential, especially by determining the presence and level of major vessel involvement by imaging before surgical treatment, which can contribute to the choice of treatment strategy.

Computed tomography (CT) plays the same critical role as the magnetic resonance imaging (MRI) in staging of STSs. There was no difference between CT and MRI in determining tumor involvement of muscle, bone, joints, neurovascular structures, or major vessel, and the combined interpretation of CT and MRIs did not improve accuracy for staging of STSs.[4,5] Contrast-enhanced axial images (CEAIs) in the arterial phase and traditional postprocessing techniques used with CEAI data, such as volume rendering (VR), can provide important information for preoperative planning of STSs. Verga et al[6] showed that contrast-enhanced CT and VR are effective in depicting adjacent major tumoral vascular involvement. Li et al[7] reported that postcontrast CT images had 100% sensitivity, 83.3% specificity, 87.5% positive predictive value (PPV), 100% negative predictive value (NPV), and 92.3% accuracy in the detection of vascular invasion, and VR had 71.4% sensitivity, 100% specificity, 100% PPV, 75% NPV, and 84.6% accuracy in the detection of vascular invasion. However, the previously mentioned methods are insufficient for clinical decision-making because these methods cannot show the spatial relationship between the lesions and the adjacent major vessels.

Cinematic rendering (CR), a new three-dimensional (3D) technique for CT image postprocessing, presents a photorealistic appearance of CT image data, with the potential to more accurately depict anatomic details and allow perception of shapes and soft tissue structures.[8–10] It allows for a more intuitive understanding of the spatial anatomical structures around tumors,

especially the spatial relationship between the lesions and the adjacent major vessels.[11,12] Thus, CR may play a crucial role in preoperative planning and clinical decision-making for STSs of the extremities.

The purpose of this study was to assess the value of CR from CT data in comparison with CEAI and VR in evaluating the relationship between deep STSs of the extremities and the adjacent major vessels.

MATERIALS AND METHODS

This was a single-center retrospective study that followed the Declaration of Helsinki and good clinical practice guidelines. This retrospective study was approved by the local medical ethics committee. The requirement for written informed consent was waived by the institutional review board.

Patients

A total of 55 consecutive patients with deep soft tissue tumors of the extremities were retrospectively included from January 2013 to June 2016. The inclusion criteria were as follows:
(1) Age 18 years or older.
(2) Presence of deep soft tissue tumors, which were defined as lesions located in the subfascial space, muscle, or muscle space, as well as adjacent to the bone.
(3) Completion of preoperative CT examinations, including unenhanced and enhanced scans, before fine-needle biopsy.

The exclusion criteria were as follows:
(1) An extended interval (more than 4 weeks) between preoperative CT examination and surgery (n = 2).
(2) Incomplete CT image information (n = 7).
(3) Surgical histopathological findings showing that the lesions were not STSs (n = 2).
(4) Diffusely distributed lesions involving multiple tissue layers, which made it difficult to determine the boundary of lesions and the relationships with large blood vessels and bones (n = 1).

Based on the previous inclusion criteria and exclusion criteria, a total of 43 patients were finally included (Fig. 1).

Computed Tomography Protocols

CT angiography examinations were performed using a 128-slice CT scanner (SOMATOM Definition AS+; Siemens Medical Solutions, Germany) with a standardized protocol. Patients were placed in the supine position on a CT scan table. An unenhanced spiral acquisition of the extremities was planned to include the tumors and at least one adjacent joint with the following parameters: tube voltage, 120 kV; tube current, 100 mAs; collimator width, 128×0.6 mm; slice thickness, 5 mm; slice spacing, 5 mm; and matrix size, 512×512. Contrast bolus tracking was used with a trigger threshold of 100 HU over the region of interest. The trigger point was located in the aortic arch, abdominal aorta, or iliac artery (depending on the tumor location) with the following parameters:
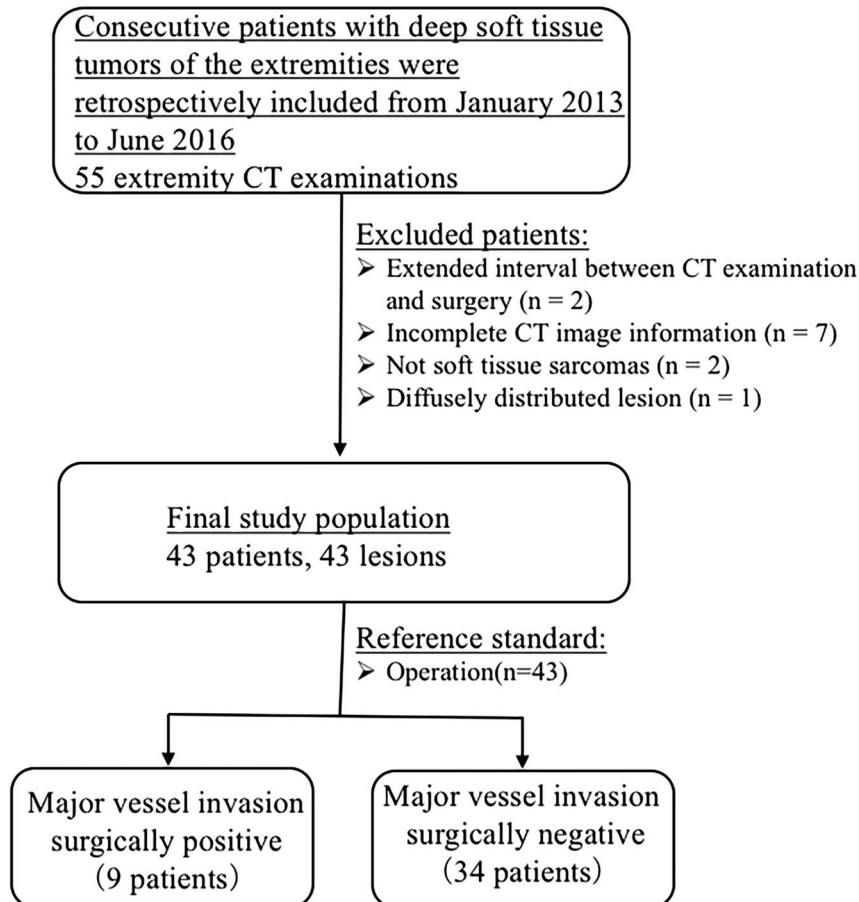

FIGURE 1. Flowchart of the study population.

tube voltage, 120 kV; tube current, 100 mAs; collimator width, 128 × 0.6 mm; pitch, 0.8; gantry rotation speed, 0.5 seconds; and variable field of view (depending on the size of the limb). Reconstruction and additional postprocessing were performed by a radiologist on a reformatting workstation (Syngo Via VB10; Siemens Healthcare, Forchheim, Germany). A nonionic contrast agent (Ultravist 300; Bayer Schering Pharma AG, Berlin, Germany) was injected with antecubital venous access at a flow rate of 4.0 mL/s. A total of 80 to 120 mL (1.5 mL per kg of body weight) was injected with a CT-compatible power injector (Bracco ACIST EZEM; Empower CT angiography) followed by injection of 30 mL of saline solution at the same rate. The scan ranges of unenhanced and enhancement images were consistent.

Three-Dimensional Image Postprocessing Methods

The raw imaging data of the CT-enhanced arterial phase scan were transferred for 3D postprocessing techniques (Syngo Via VB10; Siemens Healthcare). Volume rendering and CR images were reconstructed by an experienced skeletal radiologist (Reader 1, with 9 years of experience).

The VR reconstruction parameters, including regions of interest, were selected automatically based on the software presettings and were customized for extremity and CT angiographies. Segmental evaluation was performed by including only the regions of interest instead of evaluating the whole data set if the coverage was long, because it was in run-off studies. In addition to displaying vascular anatomy, VR reconstruction of extremities also showed osseous anatomy, which was essential for surgical planning. The CR reconstruction parameters were also selected automatically by the software presetting named Abdshaded B, which included the following settings: diffuse, 0.5; specular, 0.5; lightmap eucalyptus grove, grey; aperture, tiny; focal plane, center; albedo, 0.85; surface definition, 10; and resolution, 512 × 512.

Image Review

All images were prospectively evaluated by 2 experienced musculoskeletal radiologists (reader 1 with 9 years of experience and reader 2 with 17 years of experience). At the beginning of the study, the 2 readers were provided with hands-on instruction that clearly explained the relationship between the tumors and adjacent major vessels on the 3 types of CT images (CEAI, VR, and CR) used in this study. The definitions of the relationships on CEAI, VR, and CR were provided by referring to the literature.[6,13,14] Contrast-enhanced axial images were used to classify the relationship between the mass and the major vessels: (*a*) type 1: distance of the mass from the major vessel of greater than 1 cm; (*b*) type 2: mass adjacent to the major vessel with evidence of a thin adipose film interposition; (*c*) type 3: mass adjacent to vessel without adipose film interposition; and (*d*) type 4a: vessel partially encased and type 4b: totally encased in the lesion.[4] Volume rendering and CR were used to classify the relationship between tumors and major vessels as follows: type 1: normal route of the artery, without stenosis or occlusion interruption; type 2: vascular displacement; type 3: vascular stenosis; and type 4: vascular occlusion.[13,14] For each observation, each reader was blinded to the findings recorded by the other reader. Reader 1 repeated the image review of the relationship within a month of the previous assessment by following the same procedure. At the end of this process, most disagreements in the definitions of each type of relationship were discussed until a consensus was reached. On a few occasions when a consensus could not be reached by the 2 readers, a third reader, who was a more experienced radiologist and independent from the first two in the image review section, was invited to make the final judgment.

Reference Standard

Computed tomography evaluations and biopsies were performed for all patients, and the surgeons were aware of the results of the CT imaging evaluations before the surgery because of ethical reasons. During the surgery, the surgeons had to determine the relationship between the tumors and their adjacent major vessels, and their findings were considered as the reference standard. If the surgeons failed to dissect the adjacent major vessels from the tumors, further vascular surgery or amputation was necessitated, which was considered to indicate surgically positive findings for major vessel invasion. Surgically positive findings were also considered if the adjacent vessels adhered to or encased by the tumors could be separated. Surgically negative findings were considered if normal tissue could be found between the vessels and the tumors and the adjacent major vessels could be removed from the tumors.

Statistical Analysis

The statistical analyses were performed with R 3.4.0 (http://www.R-project.org). Cohen κ statistics and 95% confidence intervals (CIs) were used to assess the intrareader and interreader agreement for the type of relationship between tumors and adjacent major vessels on the 3 types of CT images (CEAI, VR, and
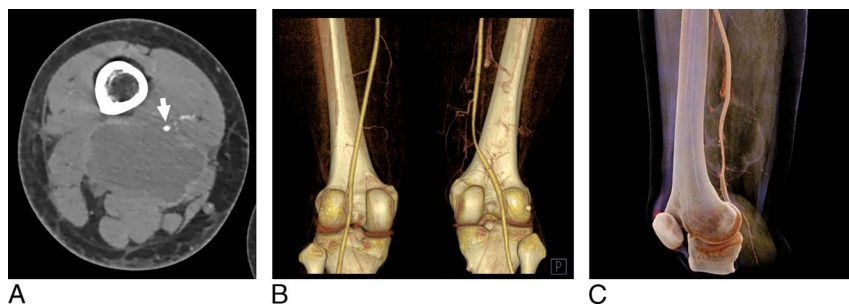
FIGURE 2. Contrast-enhanced CT image showing an intramuscular mass in the lower segment of the right thigh in a 25-year-old woman. The histological diagnosis was myofibroblastoma of soft tissue. A, Contrast-enhanced axial imaging: the mass has a well-defined margin and a maximum diameter of 6.5 cm, and the femoral artery (arrow) is totally enclosed by the mass (type 4b). B, Optimization of mass display and longitudinal extent with VR. The femoral artery is narrow, and the shape is irregular but still continuous (type 3). C, Cinematic rendering shows more natural and photorealistic anatomic details, depicting the narrowing of the femoral artery due to complete entrapment by the mass (type 3). Figure 2 can be viewed online in color at www.jcat.org.
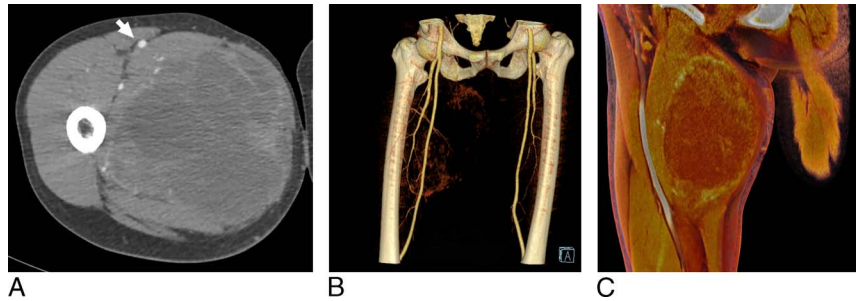
FIGURE 3. Contrast-enhanced CT image showing a large intramuscular mass in the upper segment of the right thigh in a 51-year-old man. The histological diagnosis was undifferentiated sarcoma. A, Contrast-enhanced axial imaging: the mass grows in the vastus medialis muscle with a maximum diameter of 12.4 cm, and the contrast enhancement is mildly heterogeneous and regular; the femoral artery (arrow) is dislocated by the mass, and normal tissues are interposed with a spacing >1 cm (type 1). B, Volume rendering: femoral artery is running in a natural and well-filled manner, with no abnormalities (type 1). C, Cinematic rendering shows the relationship between the mass and the femoral artery with exquisite detail, and the femoral artery is normal with a regular shape (type 1). Figure 3 can be viewed online in color at www.jcat.org.

CR). The κ values were interpreted as follows: poor agreement, 0.01 to 0.20; fair agreement, 0.21 to 0.40; moderate agreement, 0.41 to 0.60; good agreement, 0.61 to 0.80; and excellent agreement, 0.81 to 0.99.

Mean values ± standard deviations were provided for normally distributed variables. Frequencies were provided for categorical data. The χ^2 test was used to compare the categorical data in the 2 groups.

The intraoperative findings for vascular invasion were considered as the reference standard. The sensitivity, specificity, PPV, NPV, and accuracy of CEAI, VR, and CR were calculated for the presence of tumoral invasion of adjacent major vessels. The receiver operating characteristic (ROC) curve was plotted and the area under the curve (AUC) was calculated to discriminate the presence of tumoral invasion. The consistency of different ROC values was examined by the DeLong test. The test level was $\alpha = 0.05$, and $P < 0.05$ was considered statistically significant.

RESULTS

Patient Characteristics

A total of 43 patients (age, 49.51 ± 18.22 years) were involved in the study. Among these patients, 20.93% (9/43) showed surgically positive findings for tumor invasion of adjacent major vessels (Fig. 2), and 79.07% (34/43) showed surgically negative findings (Fig. 3). The detailed clinical characteristics are listed in Table 1.

Repeatability for the 3 Types of CT Images

The intrareader and interreader agreement values for assessment of the relationship between tumors and adjacent major vessels on the 3 types of CT images are shown in Table 2. Intrareader agreement values on CEAI, VR, and CR were all excellent (0.984 [95% CI = 0.953–1.000], 0.934 [95% CI = 0.846–1.000], and 0.914 [95% CI = 0.796–1.000]). However, CEAI showed greater interreader agreement than VR and CR (0.969 [95% CI = 0.927–1.000] vs 0.804 [95% CI = 0.682–0.926] and 0.761 [95% CI = 0.590–0.932]).

Comparison of the Diagnostic Performance of the 3 Types of CT Images

The relationship between tumors and adjacent major vessels of 43 patients with deep STSs of the extremities on the 3 types of CT images is summarized in Supplemental Digital Content 1, http://links.lww.com/RCT/A77. There were all statistically significant difference in the relationship on the 3 types of CT images between the major vessel invasion surgically negative group and positive group (all $P < 0.05$). Receiver operating characteristic analysis demonstrated that for CEAI, the optimal criterion was a type 3 or higher. For both VR and CR, the optimal criterion was type 2 or higher. The performance with each optical scale stratified by the 3 types of CT images for determination of tumoral invasion in adjacent major vessels is demonstrated in Table 3 and Figure 4.

In comparison with CEAI and VR, CR showed lower AUC (0.770 [95% CI = 0.582–0.957]), accuracy (0.698 [95% CI = 0.539–0.828]), sensitivity (0.778 [95% CI = 0.402–0.960]),

TABLE 1. Clinical Characteristics of the 43 Patients

Characteristic	n (%)
Sex	
Male	25/43 (58)
Female	18/43 (42)
Age, mean (SD), y	49.51 (18.22)
Tumor size, mean (SD), cm	11.87 (6.47)
Histological subtype	
Fibrosarcoma	12/43 (28)
Undifferentiated pleomorphic sarcoma	12/43 (28)
Liposarcoma	8/43 (18)
Malignant peripheral nerve sheath tumor	5/43 (11)
Vascular sarcoma	2/43 (5)
Synovial sarcoma	2/43 (5)
Leiomyosarcoma	2/43 (5)
Location	
Thigh	32/43 (74)
Shank	5/43 (12)
Upper arm	3/43 (7)
Forearm	3/43 (7)
Stage	
I	12/43 (28)
II	14/43 (32)
III	12/43 (28)
IV	5/43 (12)
Histological grade	
G1	11/43 (26)
G2	19/43 (44)
G3	13/43 (30)

TABLE 2. Intrareader and Interreader Agreement for the Relationship Between Tumors and Adjacent Major Vessels on 3 Types of CT Images

	κ Coefficients	
Image Type	**Intrareader (n = 43)**	**Interreader (n = 43)**
CEAI	0.984 (0.953–1.000)	0.969 (0.927–1.000)
VR	0.934 (0.846–1.000)	0.804 (0.682–0.926)
CR	0.914 (0.796–1.000)	0.761 (0.590–0.932)

Data in parentheses are 95% CIs.

FIGURE 4. The ROC curves of the 3 types of CT images in determining major vessel invasion. Figure 4 can be viewed online in color at www.jcat.org.

specificity (0.676 [95% CI = 0.494–0.820]), PPVs (0.389), and NPVs (0.920) for vascular invasion diagnosis; the accuracy, sensitivity, specificity, PPVs, and NPVs increased to 0.767 [95% CI = 0.614–0.882], 0.889 [95% CI = 0.504–0.994], 0.735 [95% CI = 0.553–0.864], 0.471, and 0.962 for both CEAI and VR, whereas AUC increased to 0.922 [95% CI = 0.830–1.000] for CEAI and 0.858 [95% CI = 0.711–1.000] for VR. The results were not statistically significant (all $P > 0.05$).

DISCUSSION

The main finding of this study was that CR yielded a similar accuracy (69.8%), sensitivity (77.8%), specificity (67.6%), PPV (38.9%), and NPV (92.0%) as CEAI and VR in the detection of the adjacent major vascular invasion in patients with deep STSs of the extremities. To our knowledge, this is a pioneering finding indicating the value of CR in evaluating the relationship between the deep STSs of the extremities and adjacent major vessels.

The accuracy of CEAI and VR in this study was less than in previous studies.[7,13,15] This difference might be due to the location of the lesions assessed in our study. These lesions were located in the deep soft tissues of the extremities rather than superficial soft tissues, which were more prone to cause adjacent vascular displacement and even reduction of the arterial lumen, or result in disappearance of adipose film interposition. These factors can enhance the relationship between tumors and adjacent major vessels, leading to a lower PPV for adjacent major vascular invasion. Our results also showed that the diagnostic accuracies of CR were lower than that of CEAI and VR, which would be caused by the lack of training of these radiologists.

Interestingly, our data demonstrated that the intrareader agreement for CR was excellent (91.4%), similar to that for CEAI (98.4%) and VR (93.4%), where the interreader agreement for CR was good (76.1%), similar to that for VR (80.4%) but lower than that for CEAI (96.9%). This may be related to variations in the understanding of the types of relationships between tumors and adjacent major vessels on CR and VR among different
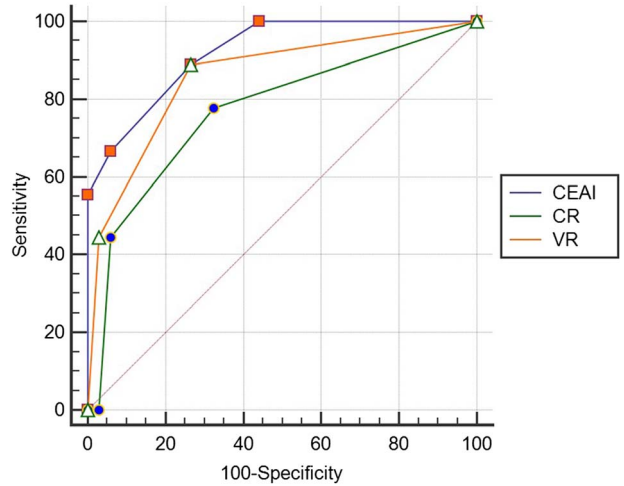
radiologists, because the 2 readers were only provided with hands-on instruction regarding the types of relationships on the 3 types of CT images (CEAI, VR, and CR) but not trained together systematically. Therefore, radiologists should receive training for identification of the relationship between tumors and adjacent major vessels on CR before the technique can be used in clinical practice.

Our data demonstrated that CR offered no statistically significant disadvantages over CEAI and VR in the detection of adjacent major vascular invasion in cases of deep STSs of the extremities. Cinematic rendering is a recently introduced novel 3D technique for postprocessing CT image data. The existing literature claimed that CR shows the best visualization for high-density and high-contrast structures such as contrast-enhanced vessels and simultaneously provides a more natural depiction of the rendered data.[8–11,16–25] More importantly, CR allows for a more intuitive understanding of the spatial anatomical structures around tumors, especially the spatial relationship between the lesions and the adjacent major vessels.[11,12] However, to our knowledge, there is no literature on the advantages and disadvantages of CR over conventional 2D images and VR for CT imaging data, which is necessary to assess a new technology. As a preliminary study, our study results provide initial evidence that CR may have some possible disadvantages such as the lower PPV for adjacent major vascular invasion, which were not statistically significant but clinically significant, but further studies are required to validate these findings.

TABLE 3. Performance of the 3 Types of CT Images for Diagnosis of Major Vessel Invasion

	Image Type			*P*		
Diagnostic Variable	**CEAI**	**VR**	**CR**	**CEAI vs VR**	**CEAI vs CR**	**VR vs CR**
AUC	0.922 (0.798–0.981)	0.858 (0.718–0.945)	0.770 (0.616–0.884)	0.423	0.097	0.169
Accuracy	0.767 (0.614–0.882)	0.767 (0.614–0.882)	0.698 (0.539–0.828)	1.000	0.626	0.626
Sensitivity	0.889 (0.504–0.994)	0.889 (0.504–0.994)	0.778 (0.402–0.960)	1.000	1.000	1.000
Specificity	0.735 (0.553–0.864)	0.735 (0.553–0.864)	0.676 (0.494–0.820)	1.000	0.790	0.790
PPVs	0.471 (0.230–0.722)	0.471 (0.230–0.722)	0.389 (0.173–0.643)	1.000	0.884	0.884
NPVs	0.962 (0.804–0.999)	0.962 (0.804–0.999)	0.920 (0.740–0.990)	1.000	0.972	0.972

Data in parentheses are 95% CIs.

Our study also has some limitations. First, the sample size was small. Twelve patients were excluded from our initial population because of the exclusion criteria, yielding a small but homogeneous population. Second, caution should be exercised in interpreting the absolute statistical values because of comparatively few cases of the adjacent major vascular invasion.

In conclusion, although not statistically significant, CR was less accurate and showed lower interreader agreement for vascular invasion of STSs compared with traditional contrast-enhanced axial CT images. Although cinematic rendering may allow for more detailed visualization and surgical planning, it should be combined with traditional imaging modalities for evaluation of vascular invasion.

REFERENCES

1. Callegaro D, Miceli R, Bonvalot S, et al. Development and external validation of two nomograms to predict overall survival and occurrence of distant metastases in adults after surgical resection of localised soft-tissue sarcomas of the extremities: a retrospective analysis. *Lancet Oncol.* 2016; 17:671–680.

2. Calvo FA, Sole CV, Cambeiro M, et al. Prognostic value of external beam radiation therapy in patients treated with surgical resection and intraoperative electron beam radiation therapy for locally recurrent soft tissue sarcoma: a multicentric long-term outcome analysis. *Int J Radiat Oncol Biol Phys.* 2014;88:143–150.

3. von Mehren M, Randall RL, Benjamin RS, et al. Soft tissue sarcoma, version 2.2016, NCCN Clinical Practice Guidelines in Oncology. *J Natl Compr Canc Netw.* 2016;14:758–786.

4. Panicek DM, Gatsonis C, Rosenthal DI, et al. CT and MR imaging in the local staging of primary malignant musculoskeletal neoplasms: report of the Radiology Diagnostic Oncology Group. *Radiology.* 1997;202:237–246.

5. Tzeng CW, Smith JK, Heslin MJ. Soft tissue sarcoma: preoperative and postoperative imaging for staging. *Surg Oncol Clin N Am.* 2007;16: 389–402.

6. Verga L, Brach Del Prever EM, Linari A, et al. Accuracy and role of contrast-enhanced CT in diagnosis and surgical planning in 88 soft tissue tumours of extremities. *Eur Radiol.* 2016;26:2400–2408.

7. Li Y, Zheng Y, Lin J, et al. Evaluation of the relationship between extremity soft tissue sarcomas and adjacent major vessels using contrast-enhanced multidetector CT and three-dimensional volume-rendered CT angiography: a preliminary study. *Acta Radiol.* 2013;54:966–972.

8. Eid M, De Cecco CN, Nance JW Jr, et al. Cinematic rendering in CT: a novel, lifelike 3D visualization technique. *AJR Am J Roentgenol.* 2017;209:370–379.

9. Johnson PT, Schneider R, Lugo-Fagundo C, et al. MDCT angiography with 3D rendering: a novel cinematic rendering algorithm for enhanced anatomic detail. *AJR Am J Roentgenol.* 2017;209:309–312.

10. Glemser PA, Engel K, Simons D, et al. A new approach for photorealistic visualization of rendered computed tomography images. *World Neurosurg.* 2018;114:e283–e292.

11. Rowe SP, Chu LC, Fishman EK. Evaluation of stomach neoplasms with 3-dimensional computed tomography: focus on the potential role of cinematic rendering. *J Comput Assist Tomogr.* 2018;42:661–666.

12. Rowe SP, Gorin MA, Allaf ME, et al. Photorealistic 3-dimensional cinematic rendering of clear cell renal cell carcinoma from volumetric computed tomography data. *Urology.* 2018;115:e3–e5.

13. Thevenin FS, Drape JL, Biau D, et al. Assessment of vascular invasion by bone and soft tissue tumours of the limbs: usefulness of MDCT angiography. *Eur Radiol.* 2010;20:1524–1531.

14. Feydy A, Anract P, Tomeno B, et al. Assessment of vascular invasion by musculoskeletal tumors of the limbs: use of contrast-enhanced MR angiography. *Radiology.* 2006;238:611–621.

15. Argin M, Isayev H, Kececi B, et al. Multidetector-row computed tomographic angiography findings of musculoskeletal tumors: retrospective analysis and correlation with surgical findings. *Acta Radiol.* 2009;50:1150–1159.

16. Dappa E, Higashigaito K, Fornaro J, et al. Cinematic rendering - an alternative to volume rendering for 3D computed tomography imaging. *Insights Imaging.* 2016;7:849–856.

17. Rowe SP, Johnson PT, Fishman EK. Initial experience with cinematic rendering for chest cardiovascular imaging. *Br J Radiol.* 2018; 91:20170558.

18. Rowe SP, Meyer AR, Gorin MA, et al. 3D CT of renal pathology: initial experience with cinematic rendering. *Abdom Radiol (New York).* 2018;43: 3445–3455.

19. Ebert LC, Schweitzer W, Gascho D, et al. Forensic 3D visualization of CT data using cinematic volume rendering: a preliminary study. *AJR Am J Roentgenol.* 2017;208:233–240.

20. Rowe SP, Zinreich SJ, Fishman EK. 3D cinematic rendering of the calvarium, maxillofacial structures, and skull base: preliminary observations. *Br J Radiol.* 2018;91:20170826.

21. Rowe SP, Fritz J, Fishman EK. CT evaluation of musculoskeletal trauma: initial experience with cinematic rendering. *Emerg Radiol.* 2018;25:93–101.

22. Rowe SP, Johnson PT, Fishman EK. MDCT of ductus diverticulum: 3D cinematic rendering to enhance understanding of anatomic configuration and avoid misinterpretation as traumatic aortic injury. *Emerg Radiol.* 2018;25:209–213.

23. Rowe SP, Zimmerman SL, Johnson PT, et al. Evaluation of Kawasaki's disease-associated coronary artery aneurysms with 3D CT cinematic rendering. *Emerg Radiol.* 2018;25:449–453.

24. Rowe SP, Fishman EK. Coronary artery to pulmonary artery fistula visualized with 3D cinematic rendering. *J Cardiovasc Comput Tomogr.* 2018;12:166–167.

25. Rowe SP, Johnson PT, Fishman EK. Cinematic rendering of cardiac CT volumetric data: principles and initial observations. *J Cardiovasc Comput Tomogr.* 2018;12:56–59.